A SIMULATION OF EARTHQUAKE AMPLIFICATION SPECTRA FOR SOUTHERN CALIFORNIA SITES

by

Donald A. Lacer [1]

ABSTRACT

A mathematical model is developed for estimating the maximum ground motion to be expected at a given site in a given time period. More than 2,000 simulated earthquakes are generated using Monte Carlo and other statistical techniques. A digital computer program is used to calculate the maximum velocity spectra at several Southern California sites due to the simulated earthquakes. It is concluded that the simulated earthquake approach is a reasonable analytic method that can be refined to yield results which will be of importance in earthquake resistant structural design.

INTRODUCTION

The problem of obtaining a realistic estimate of the maximum surface motion to be expected at any point on the earth in a given time period due to an earthquake disturbance is explored to provide a method which will yield information of use in structural design and in setting of earthquake insurance rates. One should realize that many years may elapse before earthquake phenomena are understood to the point where tangible practical results may be achieved.

Decades have been spent attempting to understand the phenomena by which earthquakes occur, trying to fully determine the methods of propagation of earthquake waves, and attempting to design structures which are earthquake proof. As yet, there is still an extremely large gap between analytic theory and empirical observation. The greatest deficiency in solving this problem is a lack of knowledge of the detailed dynamic behavior of the earth. If an effort were made to completely define the internal dynamics of the earth, knowledge of the geological structure of the earth and the analytic tools presently available would enable reasonably exact ground motions to be calculated at every point on earth. Since this is presently impractical, Monte Carlo and other statistical methods are applied to the problem of realistically generating earthquakes. Equations defining earthquake phenomena are then used to obtain a best estimate of the maximum velocity spectrum to be expected at a site in a given time period based on the mathematically generated earthquakes.

Due to the attenuation of earthquake waves with distance, it is felt that a segment of the earth can be adequately described as the complete universe, or system, if an adequate buffer zone is provided around the locations where ground motion is to be simulated. With this assumption, an area stretching from the Mexican border to San Francisco, and from well out at sea to the eastern border of California, was selected within which simulated earthquake origins were located. The resulting ground motions were computed at several sites.

---

[1] Aerospace Corporation, El Segundo, California

A block diagram of the earthquake simulation study is shown in Fig. 1. The key factors which affect the expected intensity at a given site are the generation of the earthquake, the mechanism of propagation of energy, and the ground layering characteristics. Thus, there is a transfer function based on the properties of the earth, which relates ground motion at the site to the initial vibrations at the earthquake fault. Symbolically, the transfer function has been represented by Kanai (1) as

$$U(T,q) = O(T),\ Q(T,q),\ G(T,q) \qquad (1)$$

where $U(T,q)$ is the earthquake motion at the station, and $O(T)$, $Q(T,q)$ and $G(T,q)$ represent the vibrational characteristics of the earthquake origin, of the earth's crust, and of the ground at an observing station, respectively.

The basic approach taken was to use methods of simulated sampling to attempt to realistically generate a large ensemble of earthquake epicenters. Depth of focus and magnitude were assigned to each member of the ensemble in proportion to their expected probability of occurrence in Southern California in a given time period. In this way, the earthquake inputs, $O(T)$, were specified. The best state of the art equations describing the transfer functions $Q(T,q)$ and $G(T,q)$ were next assumed and the resulting form of Eq. (1) programmed on an IBM 7090. Thousands of simulated earthquakes were used as inputs. The output was a velocity spectrum of the ground motion $U(T,q)$ at the site for each earthquake. The maximum of the velocity spectra obtained in this way is the maximum velocity spectrum that can be expected to occur at the site in a given time period.

The pertinent parameters to be chosen in the simulation were

a) Epicentral location
b) Depth of focus of earthquakes
c) Earthquake Magnitudes
d) Distance from source to site
e) Bedrock velocity at site
f) Amplification spectra at soft layered site
g) Periods of interest
h) Site locations

The confidence with which the data may be used for practical purposes, such as structural design, depends, to a great extent, upon the equations used to describe the transfer functions $Q(T,q)$ and $G(T,q)$.

SIMULATION OF EARTHQUAKE ORIGINS

EPICENTRAL LOCATION

Earthquakes in the United States are predominantly tectonic in origin. Epicentral locations, determined from seismograph recordings, have occurred near, but not necessarily directly over, known fault locations. This is explained partly by the fact that a fault, such as the San Andreas, may be strained over hundreds of miles in a single earthquake. Another source of this inconsistency is that while most of the major faults are known, there are probably many faults which have not been discovered, since many faults

do not break through to the surface. Also, locations may be obscured due to their dormancy in modern times. The dilemma at this point, then, was to determine the best way to generate the earthquake epicenters to make a representative simulation. Upon extensively comparing earthquake epicentral locations of past actual earthquakes with detailed geologic sheets of Southern California, showing major and minor fault lines, the following conclusions were reached:

(1) Several very large regions of Southern California contain weblike networks of small fault lines.

(2) Fault line location in offshore regions is unknown along the Southern California coast.

(3) Many earthquake epicenters of actual Southern California earthquakes are distributed about, if not exactly on, major fault lines.

It was therefore decided that the simulation would be of two parts. The first would consist of a number of uniformly distributed earthquake epicenters equally spaced over Southern California. These epicentral locations will simulate earthquakes originating along the myriad of short fault lines inland and also those originating from the unknown offshore faults. The second part is to locate the earthquake epicenters along the major fault lines in Southern California. This is reasonable since many epicenters can be tied directly to a major fault line. By splitting the simulation into two parts, the effects of earthquakes generated along major land faults and those generated elsewhere can be evaluated separately.

Case I: Uniformly Distributed Epicenters

The earthquake epicenters were uniformly distributed at 10 mi separations over the entire Southern California area. The epicentral matrix, then, was as shown in Fig. 2 with

$$\begin{aligned} x_o &= 0 \ (122^\circ 10' \text{W longitude}) \\ x_j &= x_{j-1} + 10 \text{ mi} \qquad (j = 1,2,3,\ldots,42) \\ y_o &= 0 \ (32^\circ 30' \text{N latitude}) \\ y_k &= y_{k-1} + 10 \text{ mi} \qquad (k = 1,2,3,\ldots,33) \end{aligned} \tag{2}$$

There were thus 1,386 equally spaced earthquake epicenters saturating the region.

Case II: Epicenters Distributed Along Major Fault Lines

By using the Monte Carlo approach in the second simulation, the earthquakes were located around major fault lines. It is known that some of the major faults have parallel trenches for some distance. Further, since actual

earthquake epicenters are spread around fault lines, not directly over them, a statistical approach to locating the earthquake epicenters is more than an approximation but is highly desirable if a realistic simulation is to be performed. With this background, geologic maps were again examined, and approximately a 2,000 mi total length of major earthquake fault lines was used in the simulation. Included among the major faults were the San Andreas, San Jacinto, Elsinore, Garlock, and Newport-Inglewood. Several other large faults in the eastern part of the state were also used. Figure 3 shows the exact fault lines. It was assumed that an earthquake might occur at any point on the fault lines with equal probability. In other words, the earthquakes would be uniformly distributed along the fault lines. Further, if the simulations were to have any statistical significance a large number of earthquakes should be generated, as in Case I, where there were 1,386 earthquakes. Therefore, 1,000 points were uniformly distributed along the earthquake fault lines of Fig. 3. Since the total length of the earthquake fault lines was 2,000 mi, each point is separated from the next by 2 mi. Next, the Monte Carlo approach was employed. It was assumed that the earthquake epicenters would be normally distributed around the earthquake fault lines. Many phenomena in nature are random, and it is practical to expect the location of earthquake epicenters around a fault line to be a normal or Gaussian process, as exemplified by the central limit theorem, Cramér (2). The Gaussian distribution is described by

$$p(x) = \frac{1}{\sigma\sqrt{2\pi}} \exp\left[-\frac{(x-\mu)^2}{2\sigma^2}\right] \qquad (3)$$

A zero mean ($\mu = 0$) was assumed in the simulation. A study of the widths of some of the parallel trenches of the major fault lines resulted in a value of 2 mi being chosen as the standard deviation, σ. One thousand normal deviates were taken at random from a table of normal deviates published by the RAND Corporation (3). Each of these normal deviates was then multipled by the standard deviation, 2 mi, to give the distance from the fault line. Next, the thousand normally distributed values were associated with one of the thousand uniformly distributed locations along the fault lines in Fig. 3. The distance of each earthquake epicenter was established by marking the proper distance normal to the fault line of each normal distribution value from its corresponding uniformly distributed point along the fault line on Fig. 3. Then, assuming the same orthogonal coordinate system defined for Case I (with origin at 122°10'W longitude and 32°30'N latitude), the coordinates of each of the thousand earthquake epicentral locations were recorded. In this way, 1,000 earthquake epicenters distributed randomly around major earthquake fault lines in the Southern California area were generated by simulated sampling, Monte Carlo methods.

Depth of Foci

In large Pacific Coast earthquakes, the foci have been on the average about 12 mi below the surface. The depth of focus of all earthquakes to be simulated in this study was therefore taken to be 12 mi.

EARTHQUAKE MAGNITUDE

The most recognized scale of earthquake magnitude is that of Gutenberg and Richter (4). The Richter-Gutenberg magnitude is a measure of the total

strain energy released by an earthquake. The magnitude number, M, is defined by

$$\log_{10}E = 9.4 + 2.14M - 0.054M^2 \quad (M > 7)$$
$$\log_{10}E = 9.4 + 1.89M \quad (M \leq 7) \tag{4}$$

where E is the total energy in ergs. This scale is not a measure of the instantaneous earthquake magnitude but is smoothed over the duration of the earthquake. It is a function of the strained length of fault and the length of time in which the grating of the surfaces takes place for a tectonic earthquake. It would be more desirable for this simulation to have an input magnitude as a function of time. However, the Gutenberg-Richter magnitude was used in this study for lack of a better measure. In the simulation, a magnitude was assigned to each earthquake based upon an estimate by Housner (5) of the number of earthquakes of a given magnitude or greater occurring in a 200 yr time period. This estimate, based on a 43 yr period of past world earthquakes and corrected to an arbitrary number of years, may be written as

$$E.N. = \frac{Y}{(43)(8.6)} \int_0^{8.7-M_1} \left[16x - (3.75)^2x^2 + (3.11)^3x^3\right] dx \tag{5}$$

where E.N. is the expected number of earthquakes in a period of Y years, which have a magnitude greater than M_1. The 200 yr period was chosen as representing the maximum time the average structure may be expected to last. The magnitudes were assigned at random to both Case I and Case II earthquake epicenters in essentially the same percentage as given for the 200 yr period.

TRANSFER FUNCTION EQUATIONS

DISTANCE FROM SOURCE TO SITE

Among the factors which might influence earthquake intensity are the distance and the azimuth between the fault strike and the source. The actual radial distance from the focus of an earthquake to the site is always greater than the straight line path, due to the bending of all ray paths toward the surface as the result of velocity anistropy with depth. The straight line path was chosen, which should result in a somewhat larger response at the site, to be consistent with a conservative approach taken throughout the study. The distance from the source to the site, then, is given by

$$r = \sqrt{(x_e - x_s)^2 + (y_e - y_s)^2 + z^2} \tag{6}$$

where x_e and y_e are the coordinates of the earthquake epicenter, x_s and y_s are the coordinates of the site, and z is the depth of focus of the earthquake, assumed to be 12 mi for all earthquakes. It was decided that for this simulation there would be no azimuthal dependency; i.e., the effect of an earthquake at a site would be a function only of its distance to a site and not its azimuth.

BEDROCK VELOCITY AT SITE

A mechanism must be specified for transporting the total kinetic energy from the earthquake origin to the base of the layering at the site. Wiggins (6) indicates that the following equation is most appropriate for the Pacific Coast:

$$V_{max} = \frac{8.1 \times 10^{-4} E^{1/3}}{(\rho_s V_s)^{1/2} r_1^{1.37}} \text{ , in./sec} \qquad (7)$$

where ρ_s and V_s, the specific density and velocity in ft/sec, respectively, are average values obtained within the boring soil, E is the total energy in ergs, and r_1 is the true travel distance in mi. The following modifications to the equation were made in the simulation:

(1) The term r_1, the true travel distance over the curved path, was replaced by r, the straight line path.

(2) The terms ρ_s and V_s, the averaged values of the layering density and velocity at the site, were replaced by ρ_b and V_b, the density and velocity of the bedrock at the potential site. This substitution should result in a more realistic estimate of the base spectrum at a given site.

SURFACE LAYERING

Basically, the earthquake causes vibrations to be transmitted in the form of elastic waves. Since the S waves are the most destructive form of wave energy propagation, only the effects of S wave energy impinging at the soft layering are considered in this simulation. Due to vertical velocity anisotropy, the ray paths describing the direction of the shear waves bend upward toward the surface. The waves may then be assumed to be applied vertically at the bottom layer of soil overlying a bedrock.

As the media within each strata are assumed continuous, the wave equation may be applied successively from layer to layer, subject to certain boundary conditions. Kanai (7), in 1950, successfully extended the solution of the wave equation to the case of viscoelastic solid bodies for a single layer case.

In 1952 Kanai (8) continued his earlier work and treated the two-layer case. Takahashi (9) contributed a graphical solution for the multilayered surface spectrum without viscosity.

The basic Takahashi equation is

$$A = \frac{2u}{u_0} = \frac{2}{\left|\cos\varphi_{n-1} + j\frac{z_{n-1}}{z_n}\sin\varphi_{n-1}\right| \cdots \left|\cos\varphi_1 + j\frac{z_1}{z_2}\sin\varphi_1\right|} \tag{8}$$

where

$$z_i = jV_i\rho_i \tag{9}$$

$$\varphi_i = \frac{\omega H_i}{V_i} + \theta_i \tag{10}$$

and

$$\theta_i = \tan^{-1}\left[\frac{z_{i-1}}{z_i}\tan\left(\frac{\omega H_{i-1}}{V_{i-1}} + \theta_{i-1}\right)\right] \tag{11}$$

Here 2u is the amplitude of the ground motion at the surface, u_0 is the amplitude of the incident wave, V_i, ρ_i, and H_i are the propagation velocity of the elastic waves, the specific density, and the thickness, respectively, of the ith layer, and ω is equal to $2\pi/T$, where T is the period of interest. A flat input spectrum (equipartition of energy) was assumed.

The author performed a FORTRAN digital computer program calculation on an IBM 7090 of the amplification spectra for the 66 strong motion accelerograph sites in Southern California, using the Takahashi equations. Site characteristics for these stations were obtained from Duke and Leeds (10).

In the simulation ground motion was computed at four sites: Vernon, Los Angeles Subway Terminal, Taft, and El Centro. These sites were chosen since many strong motion earthquakes have been recorded at these stations. In addition, the spectra of the accelerograms of earthquakes at these sites have been determined by the CIT analog computer technique (11). Los Angeles Subway Terminal and Vernon are near the center of the Southern California area being considered. They are physically located near each other but have different layering characteristics. Their relative ground motion may thus be compared.

El Centro was selected to give an indication of ground motion in the southern part of the region. Also, El Centro is located along the San Jacinto Fault and should show the effect of ground motion due to earthquakes at sites located near major faults. The results of the simulation may not be as realistic for El Centro as for the other sites, since El Centro is located near the Mexican border at the extreme edge of the simulated region. As no simulated earthquake epicenters are located below the border, the result is to minimize the ground motion to be expected at the site, since the earthquakes originating at the north of the simulated area are greatly attenuated by the large distance from the source to El Centro.

Taft is chosen since it is located near the northern edge of the simulated area, although it still has an adequate buffer zone of distance from the northern edge so that the resulting maximum ground motion should be fairly realistic.

The Takahashi equations, Eq. (8-11) were used in the computation of the amplification spectra of the layering. The site parameters, thickness, velocity, and density of the layering, used in the Takahashi equations, are summarized in Table 1. The resulting amplification factor, A, for the site at Vernon is plotted both as a function of frequency and of period in Fig. 4. This is an IBM computer printout and therefore gives a point by point rather than continuous spectrum. The computer output amplitude is digitized in discrete intervals resulting in the unsmooth appearance in obviously smooth portions of the curve. Similarly, the period and the frequency measurements are computed in finite increments. The range of periods of interest was 0.1 sec $\leq T \leq$ 2.50 sec in 0.01 sec increments. This range of periods of vibration is pertinent to the structural design problem, according to Housner (5). Because of the discrete rather than continuous computation of the amplification spectra, the value of the amplification factor may be much larger between computed periods than Fig. 4 would indicate. This is especially true at high frequencies, since the Takahashi equation includes no damping (nonviscous), and the high frequency spectra fluctuate wildly. Here high frequency corresponds to periods less than about 0.60 sec, with low frequency components corresponding to periods greater than 0.60 sec. Actually, damping due to solid viscosity will tend to smooth the amplification factor curves, particularly the high frequency components. The frequency spectrum of Fig. 4 shows that the equations are periodic. This is obscured in the period spectra since, for example, the part of the frequency spectra above 1 cps appears in the region less than 1 sec in the period spectra. Since a flat input spectrum is assumed, it can be seen that there are several dominant periods at each site due to the layering amplification spectra. A structure placed at the site would add further damping to the spectrum. The structure must be constructed to withstand the maximum expected ground motion at these dominant periods.

DISCUSSION

THE COMPUTER PROGRAM

A FORTRAN program was written, based upon the assumed transfer function equations. The coordinates of the 1,386 Case I simulated earthquakes were inserted into the IBM 7090 computer on punched cards, using Eqs. (2), with earthquake magnitudes randomly assigned in proportion to the Housner estimate. Similarly the 1,000 earthquakes of Case II were inserted in the computer. The coordinates of the Case II earthquake epicenters were extracted from Fig. 3. The computer was programmed to read in each earthquake epicentral location and magnitude in sequence and compute the distance from source to site and the energy corresponding to the assigned earthquake magnitude. With these values, Eq. (7) was solved for V_{max}, and then V_{max} was multiplied by the 0.01 sec amplification factor, which was chosen for convenience, of the site layering. The resulting velocity can then be extrapolated to any period of interest by multiplying this velocity by the ratio of the amplification factor at the 0.01 sec period to the amplification factor at the period of interest, or

$$V_{pi} = V_{0.01\ sec}\left(\frac{A_{pi}}{A_{0.01\ sec}}\right) \qquad (12)$$

where pi is the period of interest.

In this manner, the velocity at the site need only be computed at one period on the 7090 for each earthquake, saving computer time by a factor of 250. The velocity at the 0.01 sec period due to the 2,386 simulated earthquakes was computed for each of the four sites, using the bedrock velocities and densities given in Table 1 and the site coordinates and amplification factors given in Table 2.

SIMULATION RESULTS

Probability distributions of the velocities at the 0.01 sec period for both the uniform distribution and Monte Carlo simulated earthquakes for the sites at Vernon, El Centro, Taft, and Los Angeles Subway Terminal are shown in Figs. 5-8, respectively. The distributions are not the expected exponential type and, at first glance, appear to be Rayleigh distributed. In a Rayleigh distribution, the mean value is 1.25 times the standard deviation, and the peak of this distribution occurs at the standard deviation. These characteristics of the Rayleigh distribution were not found to exist in any of the eight probability distributions of Figs. 5-8. A possible explanation is that the distribution is a modified exponential distribution. Since there are far more earthquakes of relatively low magnitude, $6 \leq M \leq 6.4$, those of low magnitude far from the recording site will yield a very low velocity at the site, while those close to the site will yield a larger value. Conversely, the larger magnitude earthquakes are far fewer. Those close to the site will yield a very high velocity at the site, while those far from the site will yield a lower velocity at the site; but this lower velocity is still higher than the highest velocity produced by the lower magnitude earthquakes and is far higher than the lowest velocity produced by the lower magnitude earthquakes. In other words, the weighting introduced by the distance from the source to the site is probably responsible for the introduction of a peak into the probability distributions. The triangles in Figs. 5-8 are the highest velocities obtained due to individual earthquakes. The highest velocities at the 0.01 sec period recorded at any site ranged from 2.2 in./sec at Vernon to 12.5 in./sec at El Centro. Due to the preliminary nature of these initial results, it was felt that nothing could be gained by combining the uniform distribution and Monte Carlo results into composite probability distributions. The mean velocity of each distribution at the 0.01 sec period was calculated and is shown in Table 3. It can be seen that at each site the Monte Carlo mean velocity is greater than the mean velocity given by the uniformly distributed case. Table 3 also contains the dominant periods of the high and low frequency peaks of the amplification spectra of each site along with the corresponding amplification factor. The mean velocity at each dominant period, scaled from the 0.01 sec period mean velocity, is also indicated.

The maximum velocity at the 0.01 sec period for each distribution is shown in Table 4. It can be seen that the maximum velocity recorded at a site is approximately the same for both the Monte Carlo and uniform distribution simulations, but the maximum recorded velocity, as stated above,

varies by about an order of magnitude range between sites. Furthermore, in contrast to the mean velocity, the maximum velocity at a site was higher for the Monte Carlo case at two sites but was higher for the uniformly distributed case at the other two sites. In an identical manner to the scaling of the mean velocity, the maximum velocity at the 0.01 sec period at each site was scaled to yield maximum velocities to be expected at the various dominant high and low frequency periods of interest. It can be seen from Table 4 that velocities as large as 8 ft/sec at high frequencies and about 2 ft/sec at low frequencies were given by the simulation. It should again be mentioned that no damping terms due to solid viscosity nor to structures were included in the simulation equations; and that damping effects will have a large smoothing effect on reducing the high frequency velocity amplitudes.

To determine whether the simulation resulted in reasonable values of the maximum ground motion to be expected at a site, consider the average velocity spectra of Fig. 9, which is the average of the eight components of the four strongest ground motions recorded to date. The top curve, with no damping due to structures, shows a definite high frequency peak at about a 0.5 sec period with a velocity of about 1.3 ft/sec. The curve levels off to about 1 ft/sec velocity at lower frequencies. Since Fig. 9 shows an average value, the individual earthquake velocities may have been higher or lower than the average. Nevertheless, the maximum high frequency velocity given by the simulation, 8 ft/sec, is larger than the 1.3 ft/sec of the past actual data. The simulation resulted in a low frequency maximum velocity of 2 ft/sec, compared with an actual maximum velocity of 1 ft/sec at low frequencies. It should be emphasized that the recording instruments have only been in position since 1930, and thus there is only a very small sample of strong motion earthquakes used in the comparison. Notice also the effects of damping due to structures on the average spectra of Fig. 9. As the damping is increased to 10 percent, the high frequency peak is attenuated faster than the low frequency portion of the curve. The peak finally disappears with increased damping, and the remaining low frequency portion of the curve is higher than the high frequency part of the curve.

Although the probability distributions of velocity are plotted in Figs. 5-8, it was decided that the information was so preliminary that it would be unnecessary to calculate the probabilities that a ground motion of a given velocity at a given period would occur at a given site in a given time period. It was further felt that this type of calculation might even lead to use of these results at this time, which would be very unwise.

A comparison made by simulating an actual past earthquake and comparing the ground motion given by the simulation at the four sites with that actually recorded at the sites was not performed. The equations used in the simulation are based in part upon such comparisons. The author wished to use the best available equations, not develop new equations, since the prime purpose was to demonstrate the simulated sampling approach and not to optimize the transfer function.

CONCLUSIONS

The prime purpose of this study was to develop a method of estimating the maximum ground motion to be expected at a given site in a given time period. Based on the results of this study, it may be concluded that the

simulated earthquake approach is a reasonable analytic method. The mathematical model, based upon Eq. (1), yielded maximum ground motions at the various sites, which are on the order of the highest actual ground motions which have been recorded in Southern California. The study has highlighted the very powerful influence that the modern high speed digital computer, in conjunction with statistical techniques, can exert in generating usable data, particularly where such data would be physically impossible to obtain in any other way.

Before the results of the simulation are practical for use in structural design or the setting of earthquake insurance rates, the following areas should be examined in detail:

EPICENTRAL LOCATION

The location of the earthquake epicenters along major fault lines seems to be a good assumption in the study. However, the placing of the uniformly distributed epicenters across Southern California was an attempt to overcome the general lack of knowledge on the location of offshore fault lines and to account for the many small networks of fault lines in various sections of Southern California. Clearly, this is not an optimum placing of epicenters which might occur due to these fault lines. In a future study available information on location of these faults might be examined in more depth.

MAGNITUDE

The Richter-Gutenberg magnitude, used in the study, is a single value which corresponds to the total energy involved in the earthquake mechanism. For short, pulselike earthquakes, which many earthquakes are, this is a good measure. However, in general, an earthquake may occur over an appreciable time interval, in which the Richter-Gutenberg magnitude is inaccurate when simulating ground motion at a site. A new definition of earthquake magnitude is necessary. It is hoped that future research can be carried out on the formation of a refined measure, including the effect of the duration of a quake.

TRANSFER FUNCTION EQUATIONS

Many of the coefficients included in the transfer function equations are theoretical values with numerous assumptions involved, or are great simplifications made to make the simulation tractable, or are averaged values based on a dirth of empirical data. The transfer functions are perhaps the weakest feature of the simulation. The refinement of the transfer function equations may result in the largest improvement of the data produced in this study. Alternate forms of the transfer functions may be desirable, particularly the transfer function derived by Kanai (1):

$$v = 0.213 \times 10^{0.61M - 1.73 \log \Delta}$$

$$\times \left(1 + \left[\left\{ \frac{1+c}{1-c} \left[1 - \left(\frac{T}{T_0} \right)^2 \right] \right\}^2 + \left[\frac{0.3}{\sqrt{T_0}} \left(\frac{T}{T_0} \right) \right]^2 \right] \right)^{-1/2}, \text{ cm/sec} \qquad (13)$$

Here the predominant period of the ground, T_0, at the site must be known. This equation was not employed in the simulation due to the desirability to keep the study general, not requiring knowledge of the predominant ground period of a site. However, it might be desirable to substitute Eq. (13) for Eqs. (7) and (8-11) and compare the resulting ground motions.

DAMPING EFFECTS

No damping terms due to solid viscosity were used in Eqs. (8-11) in determining the site amplification spectra. Introduction of damping terms greatly increases the complexity of the amplification spectra equations. To make a true representation of the effects of layering at a site, the damping due to solid viscosity of the layers should be included.

STRUCTURES

The study did not include the damping effects of structures located at the site. There is a considerable effort to determine the response of structures, such as bridges, buildings, and dams, to earthquake motions. In particular, the structure will feedback energy into the layering, considerably altering the resonant characteristics of the site. As these structural interaction studies reach fruition, the effect of damping due to structures can be used to extend the usefulness of this study.

In summary, it is felt that this study has been an initial effort to simulate the maximum ground motion to be expected at a site in given time period due to earthquakes, and has resulted in a reasonable analytic approach that can in the future be refined and improved to yield results which will be of extreme importance in earthquake resistant structural design.

ACKNOWLEDGEMENTS

The author wishes to thank Professors R. B. Matthiesen and C. M. Duke of the University of California, Los Angeles, for guidance and encouragement over the period during which the simulation was conceived and performed. The records and reference material obtained from D. J. Leeds, Research Specialist, were greatly appreciated.

REFERENCES

1. Kanai, K., "An Empirical Formula for the Spectrum of Strong Earthquake Motion," Proc., Second World Conference on Earthquake Engineering, Earthquake Research Institute, July 11-18, 1960, Tokyo and Kyoto, Japan, p. 1541-1551.

2. Cramér, Harald, Mathematical Methods of Statistics, Princeton University Press, New Jersey, 1951, p. 213-232.

3. The RAND Corporation, A Million Random Digits with 100,000 Normal Deviates, The Free Press, Glencoe, Illinois, 1955.

4. Gutenberg, B. and Richter, C. F., "Earthquake Magnitude, Intensity, Energy, and Acceleration." Bull. of Seis. Soc, Vol. 46, 105-145, April 1956.

5. Housner, G. W., "Intensity of Ground Motion During Strong Earthquakes," California Institute of Technology, Technical Report, ONR Contract N60nr-244, Task 25, Project NR-081-095, August 1952.

6. Wiggins, John Henry, Jr., The Effect of Soft Surficial Layering on Earthquake Intensity, Ph. D. dissertation, Univ. of Illinois, Urbana, Illinois, May 1961.

7. Kanai, K., "The Effect of Solid Viscosity of the Surface Layer on the Earthquake Movements," Bull. of Earthquake Research Institute, Vol. 28, 31-35, 1950.

8. Kanai, K., "Relation Between the Nature of Surface Layer and the Amplitudes of Earthquake Motions," Bull. of Earthquake Research Institute, Vol. 30, 31-37, 1952.

9. Takahashi, R., "A Short Note on a Graphical Solution of the Spectral Response of the Ground," Bull. of Earthquake Research Institute, Vol. 33, 259-264, 1955.

10. Duke, C. M. and Leeds, D. J., "Site Characteristics of Southern California Strong-Motion Earthquake Stations," Univ. of California, Los Angeles, Technical Report, 62-55, Nov. 1962.

11. Alford, J. L., Housner, G. W., and Martel, R. R., "Spectrum Analysis of Strong-Motion Earthquakes," California Institute of Technology, First Technical Report, ONR-081-095, August 1951.

12. Housner, G. W., "Behavior of Structures During Earthquakes," Proc. Am. Soc. C. E., Oct. 1959.

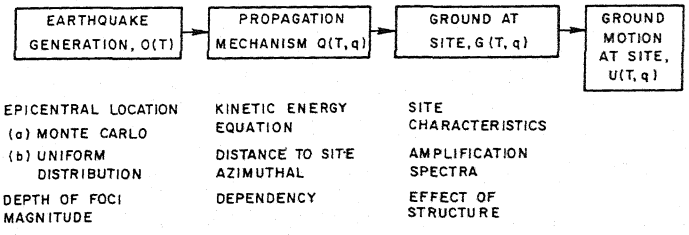

FIG. 1. EARTHQUAKE SIMULATION STUDY

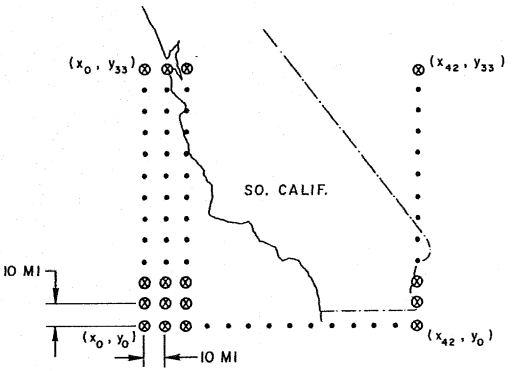

FIG. 2 EARTHQUAKE EPICENTER LOCATION FOR UNIFORMLY DISTRIBUTED CASE

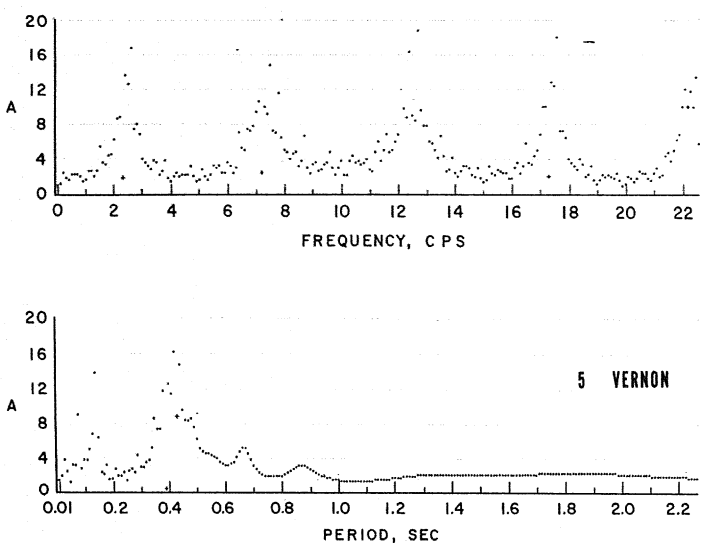

FIG. 4. AMPLIFICATION SPECTRA: VERNON
(FROM PROF. R. B. MATTHIESEN OF UCLA)

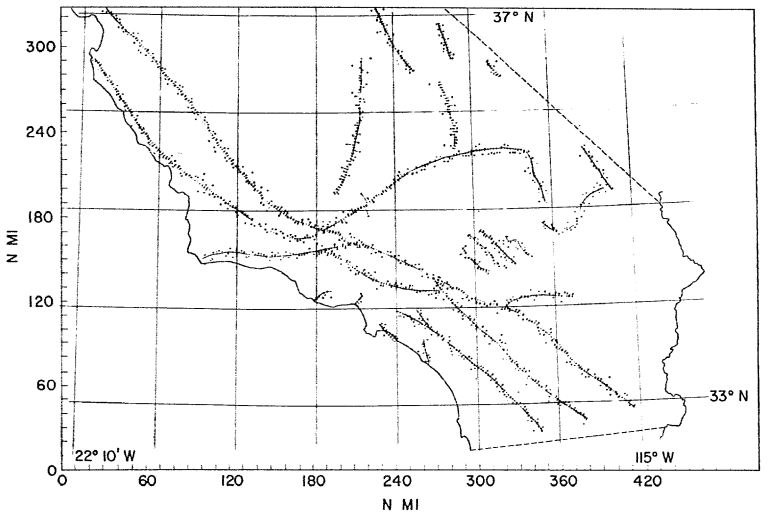

FIG. 3. EPICENTRAL LOCATION ALONG MAJOR FAULT LINES

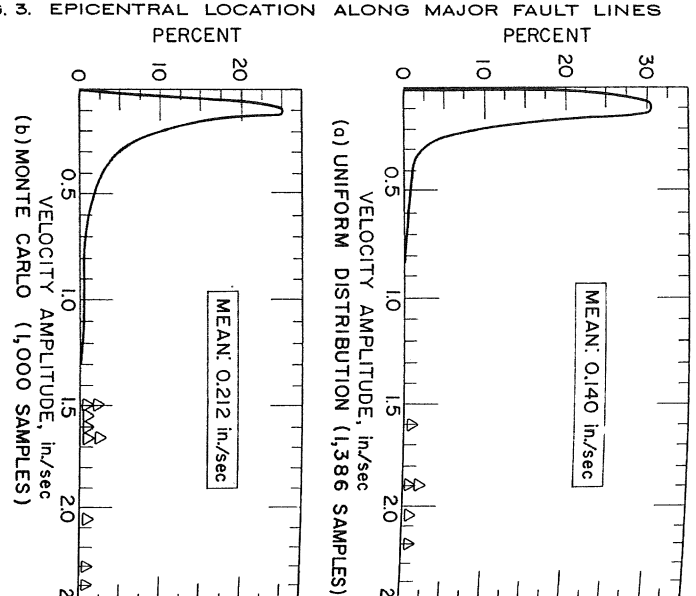

FIG. 5. PROBABILITY DISTRIBUTION - VERNON; T = 0.01 SEC

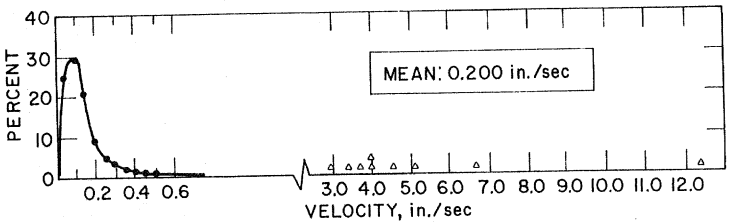

(a) UNIFORM DISTRIBUTION; 1386 SAMPLES

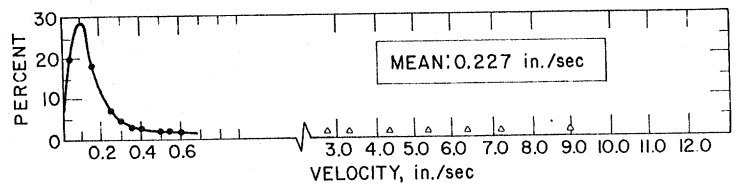

(b) MONTE CARLO; 1000 SAMPLES

FIG. 6. PROBABILITY DISTRIBUTION FOR EL CENTRO; T = 0.01 SEC

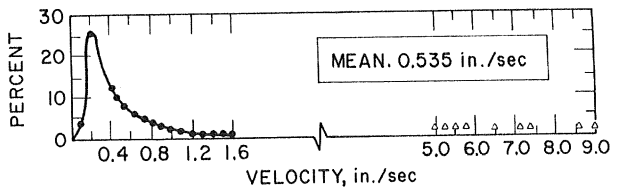

(a) UNIFORM DISTRIBUTION; 1386 SAMPLES

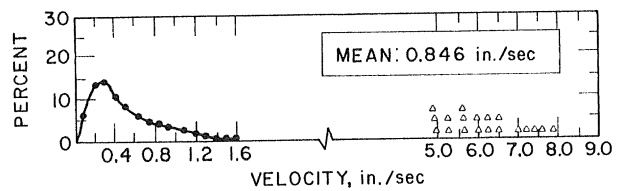

(b) MONTE CARLO; 1000 SAMPLES

FIG. 7. PROBABILITY DISTRIBUTION FOR LOS ANGELES SUBWAY TERMINAL; T=0.01 SEC

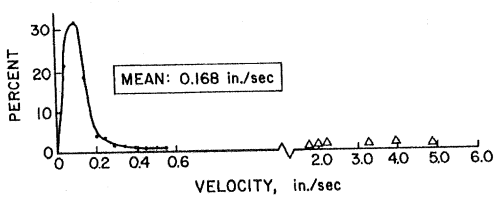

(a) UNIFORM DISTRIBUTION; 1386 SAMPLES

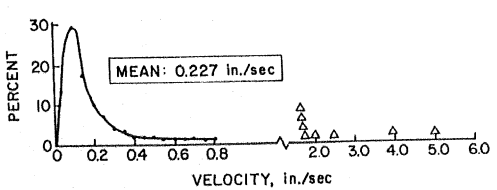

(b) MONTE CARLO; 1000 SAMPLES

FIG. 8. PROBABILITY DISTRIBUTION FOR TAFT; T = 0.01 SEC

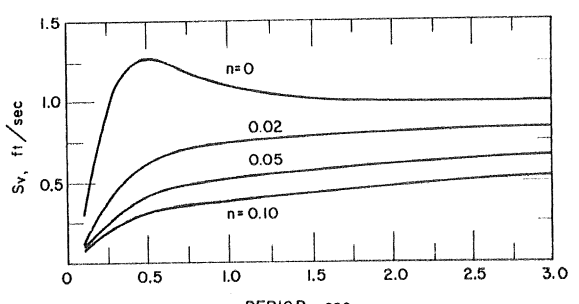

FIG. 9. AVERAGE OF EARTHQUAKE VELOCITY SPECTRA (FROM G.W. HOUSNER, REF. 12)

TABLE 1. SITE PARAMETERS

LAYER NO.	VERNON THICKNESS ft	VERNON VELOCITY FPS	VERNON DENSITY %	EL CENTRO THICKNESS ft	EL CENTRO VELOCITY FPS	EL CENTRO DENSITY %
1	40	1000	110	62	1200	125
2	160	5000	110	1738	5900	138
3	1800	7500	137	2900	7600	139
4	3000	9000	137	3800	8500	147
5	3000	12,000	148	---	---	--
BEDROCK	---	16,000	166	---	12,200	147

LAYER NO.	TAFT THICKNESS ft	TAFT VELOCITY FPS	TAFT DENSITY %	LA SUBWAY TERMINAL THICKNESS ft	LA SUBWAY TERMINAL VELOCITY FPS	LA SUBWAY TERMINAL DENSITY %
1	40	1190	105	20	1800	120
2	160	5000	140	380	3500	128
3	5500	6400	144	1600	8000	137
4	5500	7800	148	3000	9000	148
5	---	---	--	3000	9500	145
BEDROCK	---	15,500	170	---	16,000	166

TABLE 2. SITE LOCATION AND AMPLIFICATION FACTOR

SITE	x-COORDINATE MI	y-COORDINATE MI	AMPLIFICATION FACTOR, A 0.01 SEC
VERNON	230.0	108.0	1.39
EL CENTRO	381.0	38.0	2.31
TAFT	162.0	195.0	1.53
LA SUBWAY TERMINAL	228.0	120.0	5.17

TABLE 3. MEAN VELOCITY

SITE	HIGH FREQUENCY PERIOD (SEC)	HIGH FREQUENCY AMPLIFICATION FACTOR	HIGH FREQUENCY MEAN VELOCITY (in./sec) MC	HIGH FREQUENCY MEAN VELOCITY (in./sec) UD	LOW FREQUENCY PERIOD (SEC)	LOW FREQUENCY AMPLIFICATION FACTOR	LOW FREQUENCY MEAN VELOCITY (in./sec) MC	LOW FREQUENCY MEAN VELOCITY (in./sec) UD
VERNON	0.01	1.39	0.212	0.140	0.66	5.28	0.81	0.531
	0.43	28.79	4.38	2.9	0.87	3.27	0.497	0.328
	0.39	20.34	3.09	2.05	1.85	2.41	0.365	0.242
	0.14	13.87	2.12	1.40				
EL CENTRO	0.01	2.31	0.227	0.200	0.80	17.63	1.73	1.53
	0.11	11.81	1.17	1.01	0.95	9.45	0.93	0.82
	0.26	7.41	0.76	0.64	1.18	5.92	0.58	0.51
					1.57	4.31	0.44	0.37
TAFT	0.01	1.53	0.227	0.168	0.54	5.23	0.79	0.59
	0.33	27.9	4.02	2.97	0.75	4.33	0.67	0.48
	0.42	7.29	1.08	0.78	1.21	3.23	0.48	0.36
LA SUBWAY TERMINAL	0.01	5.17	0.846	0.535	1.15	7.67	1.26	0.79
	0.21	9.25	1.51	0.96	0.95	6.73	1.10	0.69
	0.14	9.00	1.48	0.94	1.63	4.78	0.77	0.50

TABLE 4. MAXIMUM VELOCITY

SITE	HIGH FREQUENCY PERIOD (SEC)	HIGH FREQUENCY AMPLIFICATION FACTOR	HIGH FREQUENCY MAXIMUM VELOCITY (in./sec) MC	HIGH FREQUENCY MAXIMUM VELOCITY (in./sec) UD	LOW FREQUENCY PERIOD (SEC)	LOW FREQUENCY AMPLIFICATION FACTOR	LOW FREQUENCY MAXIMUM VELOCITY (in./sec) MC	LOW FREQUENCY MAXIMUM VELOCITY (in./sec) UD
VERNON	0.01	1.39	2.46	2.25	0.66	5.28	9.38	8.55
	0.43	28.79	51.0	46.6	0.87	3.27	5.80	5.30
	0.39	20.34	36.1	33.0	1.85	2.41	4.27	3.90
	0.14	13.87	24.6	22.5				
EL CENTRO	0.01	2.31	8.94	12.5	0.80	17.63	68.3	95.8
	0.11	11.81	45.8	64.0	0.95	9.45	36.6	51.1
	0.26	7.41	28.7	40.3	1.18	5.92	22.9	32.0
					1.57	4.31	16.7	23.4
TAFT	0.01	1.53	5.0	4.93	0.54	5.23	17.1	16.8
	0.33	27.9	91.1	89.9	0.75	4.33	14.2	13.9
	0.42	7.29	23.7	23.4	1.21	3.23	10.6	10.4
LA SUBWAY TERMINAL	0.01	5.17	7.8	10.9	1.15	7.67	11.6	16.2
	0.21	9.25	14.0	19.5	0.95	6.73	10.2	14.2
	0.14	9.00	13.6	19.0	1.63	4.78	7.4	10.1

A SIMULATION OF EARTHQUAKE AMPLIFICATION SPECTRA FOR SOUTHERN CALIFORNIA SITES

BY D.A. LACER

QUESTION BY: G.W. HOUSNER - U.S.A.

Attention is called to the fact that Fig. 9 should be labelled "Normalized Spectra" and it must be multiplied by appropriate numerical factors in order to represent actual computed spectra.

AUTHOR'S REPLY: Professor Housner's remark concerning the labelling of Figure 9 is correct. Reference may be made to Professor Housner's paper entitled "Behaviour of Structures During Earthquakes", Proc. Am. Soc. C.E., October 1959, for the appropriate multiplication factors for Figure 9 to represent actual computed spectra.